6.9 A SIMPLIFIED APPROACH TO VVER-440 FUEL ASSEMBLY HEAD BENCHMARK

Petr Mühlbauer
Nuclear Research Institute Řež plc
250 68 Czech Republic

ABSTRACT

The VVER-440 fuel assembly head benchmark was simulated with FLUENT 12 code as a first step of validation of the code for nuclear reactor safety analyses. Results of the benchmark together with comparison of results provided by other participants and results of measurement will be presented in another paper by benchmark organisers. This presentation is therefore focused on our approach to this simulation as illustrated on the case 323-34, which represents a peripheral assembly with five neighbours. All steps of the simulation and some lessons learned are described.

Geometry of the computational region supplied as STEP file by organizers of the benchmark was first separated into two parts (inlet part with spacer grid, and the rest of assembly head) in order to keep the size of the computational mesh manageable with regard to the hardware available (HP Z800 workstation with Intel Zeon four-core CPU 3.2 GHz, 32 GB of RAM) and then further modified at places where shape of the geometry would probably lead to highly distorted cells. Both parts of the geometry were connected via boundary profile file generated at cross section, where effect of grid spacers is still felt but the effect of outflow boundary condition used in the computations of the inlet part of geometry is negligible.

Computation proceeded in several steps: start with basic mesh, standard k – ε model of turbulence with standard wall functions and 1st order upwind numerical schemes; after convergence (scaled residuals lower than 10^{-3}) and near-wall meshes local adaptation when needed, realizable k – ε of turbulence was used with 2nd order upwind numerical schemes for momentum and energy equations. During iterations, area-average temperature of thermocouples and area-averaged outlet temperature which are the main figures of merit of the benchmark were also monitored.

In this “blind” phase of the benchmark, effect of spacers was neglected. After results of measurements are available, standard validation simulations will be performed.

1. INTRODUCTION

The VVER-440 fuel assembly head blind benchmark organized by AER was selected as a part of validation procedure leading to approval of the FLUENT 12 code by Czech regulatory body (Státní úřad pro jadernou bezpečnost, SÚJB) for thermal-hydraulic analyses of nuclear reactor fuel assemblies. A simplified approach was selected since this is the first FLUENT 12 analysis of such problem in the NRI and it is envisaged that standard validation will be performed after experimental results are known.

A blind benchmark represents a very common situation of application of a CFD code to a case where experimental support is poor or nonexistent. Producers of the CFD software provide the users with some guidelines how to proceed in such situation and there are also some Best Practice Guidelines (BPG) elaborated by various groups of users. Nevertheless, any CFD code application is in some sense unique. This paper deals with our approach to such "demonstration" calculation.

After inspection of assembly head geometry supplied to us in form of a STEP file and with regard to figures of merit of the benchmark (temperatures measured by thermocouples near the assembly outlet) it was decided to separate the computational domain into two parts connected via a "boundary profile file". This decision enabled us to combine various simplifying assumptions or different computational meshes in the two parts. This step is discussed in the next section of the paper. The (steady state) computations themselves proceeded in several steps involving two models of turbulence (standard and "realizable" k – ε models) with standard wall functions and 1st and 2nd order upwind numerical schemes. Pressure-based solver and SIMPLE algorithm were selected. Since all results of the benchmark together with results of measurements will be presented in another paper by the benchmark organizers, this paper is focused only on the case 323-34 (peripheral assembly) with prescribed flow through the central tube. Moreover, our steady state computations revealed that the flow in the assembly head is very probably unsteady. We therefore performed unsteady computations starting from the steady state results. These computations are in fact the main subject of this paper.

2. SIMPLIFICATIONS OF GEOMETRY

Geometry of the VVER-440 assembly head as provided by organizers is shown in Fig. 1 (left). From the point of view of mesh generation, there are two critical parts: grid spacers near the inlet, and the catcher (a frustum with rosette-like holes) just upstream the outlet cylinder. Also, in order to have maximum versatility in distribution of hardware capability it was decided to separate the computational region into two overlapping parts: inlet region with length of 100 mm composed of the fuel pins with grid spacers, and outlet region starting 63 mm from the inlet where boundary profile was generated as shown in Fig. 1.

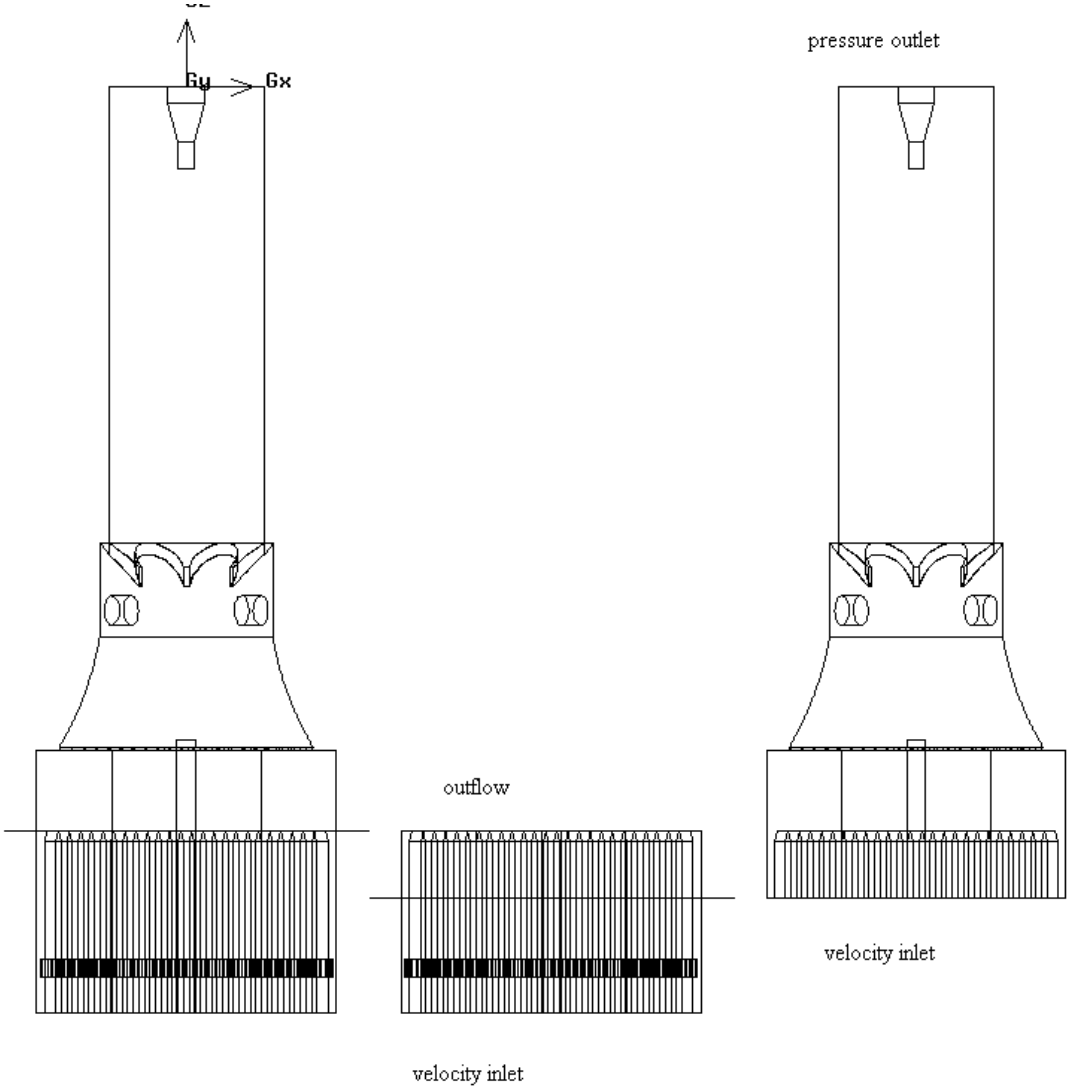

Fig. 1: Benchmark geometry and its separation into two overlapping parts with boundary conditions as indicated.

Grid spacers (Fig. 2) with length of 10 mm represent an obstacle producing a pressure drop. Their effect on coolant inter-subchannel mixing is less obvious: spacers participate in generation of turbulence in the downstream wake but prevents mixing to some degree by forcing axial flow. We therefore decided in the "blind" phase of the benchmark to neglect the spacers, so that the computations of the inlet region were performed with bare rods. Moreover, most mixing can be expected in the remaining part of the assembly so that the outlet temperatures need not be too much affected. We also replaced the frustum-shaped ends of the fuels pins by cylinders.

The original geometry of the catcher (Fig. 3) in fact prevents generation of high-quality mesh due to some problem areas connected with the rosette-like holes. The geometry was therefore slightly modified as shown in Fig. 4. It is believed that the results of the computations are not appreciably affected.

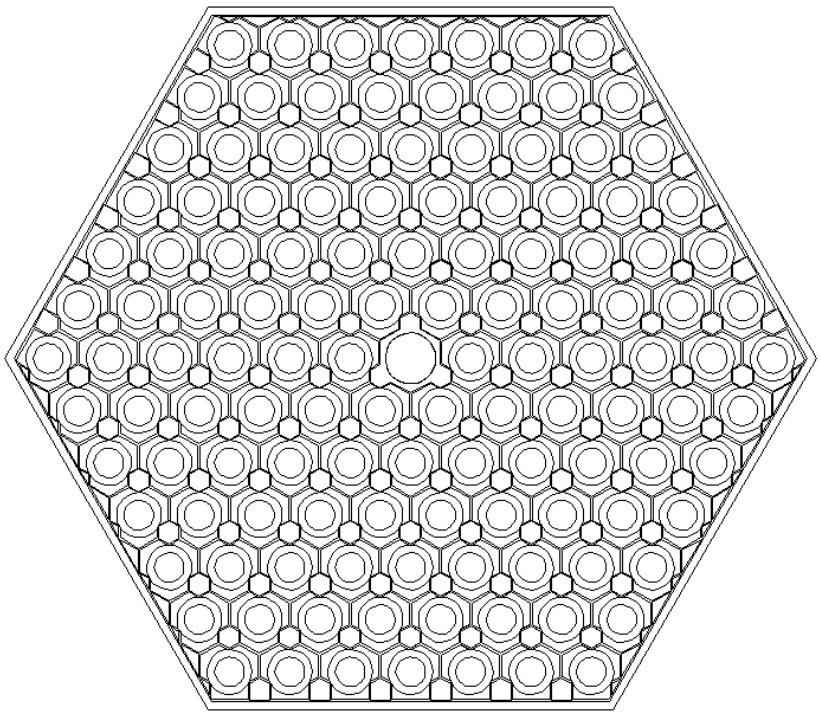

Fig. 2: Grid spacers (neglected in the “blind” step of validation procedure).

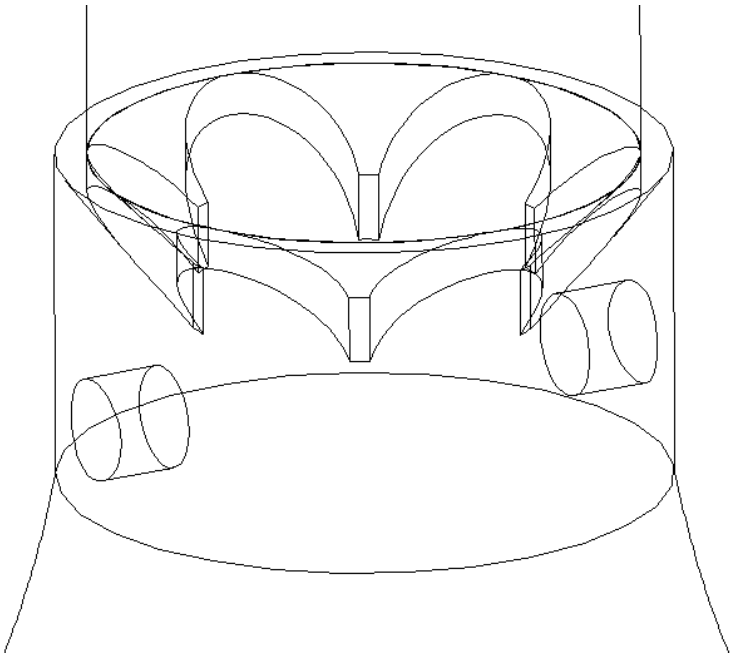

Fig. 3: Original geometry of the catcher.

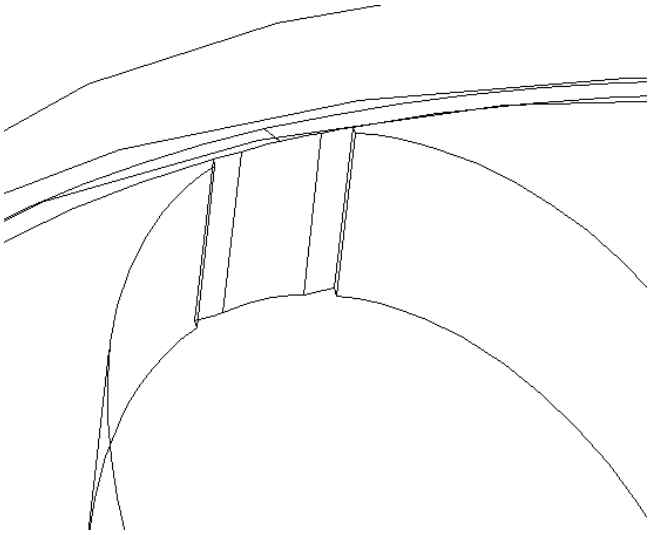

Fig. 4: Modified geometry of the catcher.

3. INLET REGION

Computational mesh in the inlet region generated by means of GAMBIT 2.4.6 pre-processor has 4 129 000 wedge and hexagonal cells with 4 layers of hexagonal cells near the solid walls as shown in Fig. 5. Thickness of the first layer of 0.1 mm led to dimensionless wall distance y^+ less than 100.

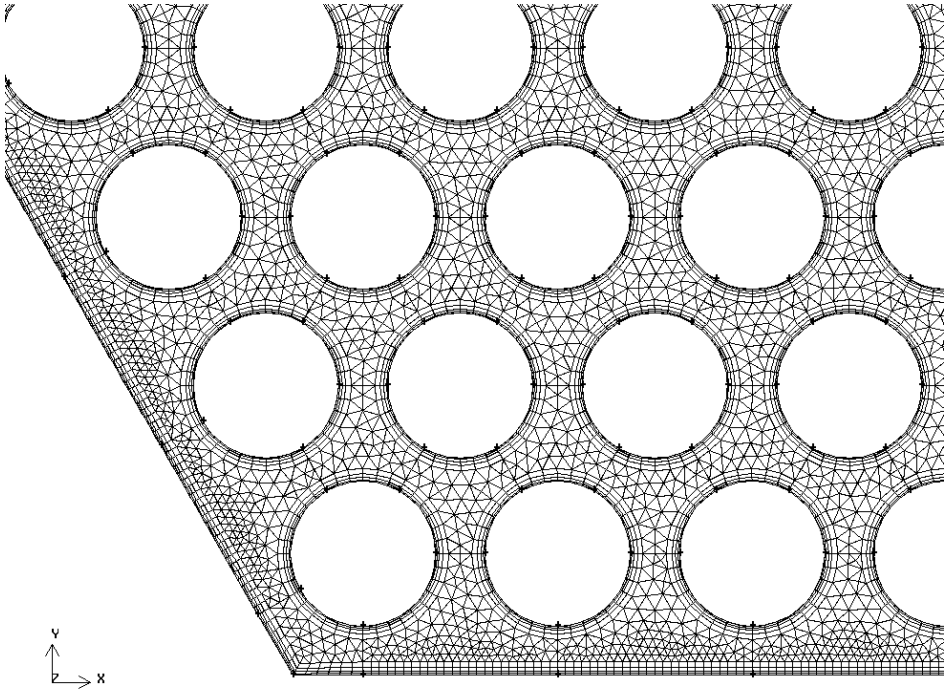

Fig. 5: Computational mesh in the inlet region.

Good convergence with scaled residuals lower than 10^{-4} even after switch to 2nd order upwind schemes for momentum and energy equations as shown in Fig. 6 can be taken as an evidence of acceptable mesh. Boundary profiles (3 components of velocity, temperature, turbulent kinetic energy and its dissipation rate) were taken for every analysed case at the distance of 63 mm from the inlet and used as inlet boundary condition for the outlet region.

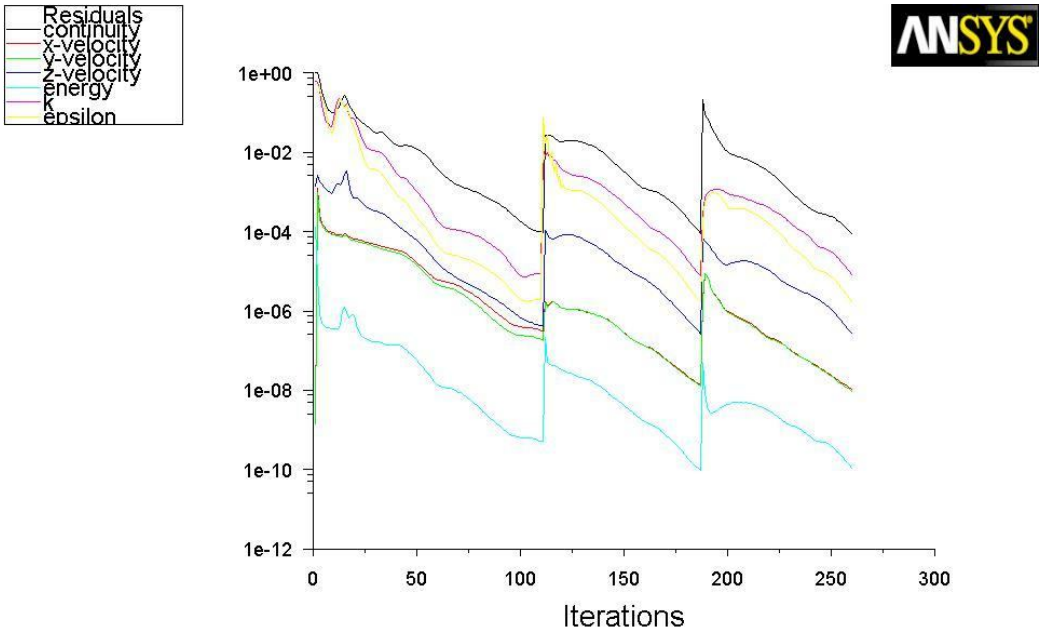

Fig. 6: Scaled residuals with switch from standard to "realizable" k – ε model of turbulence after 110 iterations and from 1st to 2nd order numerical schemes after 187 iterations.

4. OUTLET REGION

4. 1. Computational mesh

Due to complex geometry of the outlet region it was decided to separate the region into several sub-volumes which can be meshed by different algorithms. With regard to dimensionless wall distance, we generated several near-wall grids and finally started with some compromise: the basic mesh has 7 538 403 hexagonal, wedge, pyramid and tetrahedral cells and it was envisaged that in critical locations this basic mesh will be improved by local mesh adaptation. Equi-size skew (ESS) was selected as a criterion of the mesh quality with ESS $\leq$ 0.75 as an evidence of an acceptable mesh. Unfortunately we did not succeed to meet this limit; there are 238 cells with ESS higher than 0.75 (ESS_{max} = 0.82) located in the catcher, Fig. 7, and in front of the thermocouple, Fig. 8. It is obvious that such cells can negatively affect the results of computations, mainly near the thermocouple.

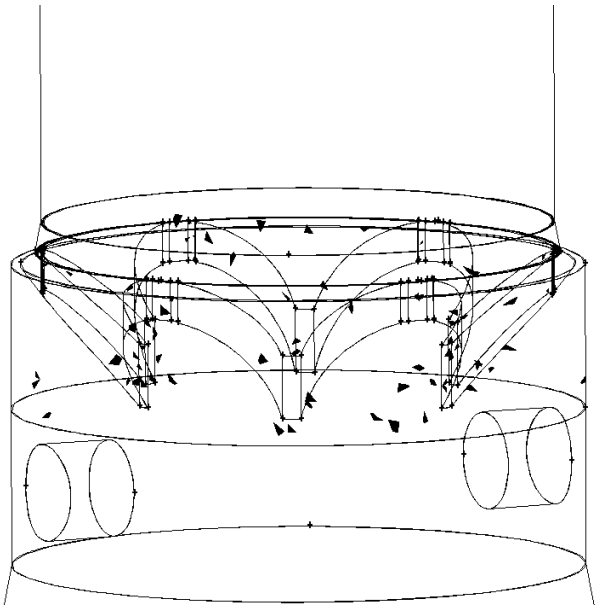

Fig. 7: Cells with ESS > 0.75 in the catcher region.

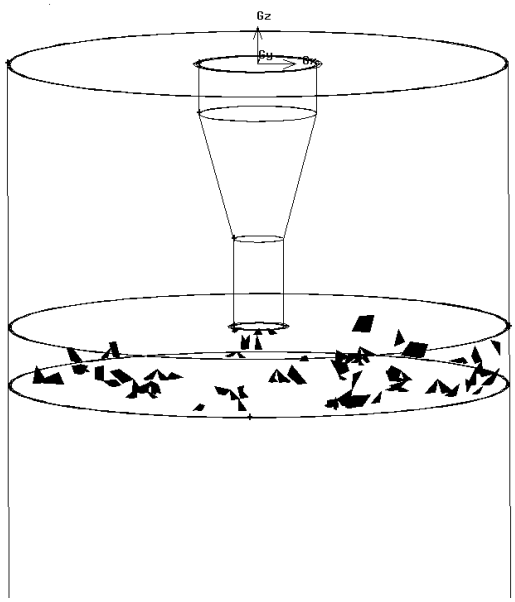

Fig. 8: Cells with ESS > 0.75 in the region of thermocouple.

4. 2. Steady state computations

Similarly to the computations of the inlet region, we started with standard k – ε model of turbulence, 1st order upwind numerical schemes and basic mesh. Local mesh adaptation was performed several times after acceptable convergence of solution in order to keep dimensionless wall distance y+ lower than 400. After 500 iterations we switched to "realizable" k – ε model of turbulence, and after 800 iteration 2nd order upwind numerical scheme for momentum and energy equations were used. The final mesh has 8 507 002 cells. Further attempts to adapt the mesh led to abnormal termination of computations.

Behaviour of scaled residuals for the case 323-34 is shown in Fig. 9. It is obvious that switch to the 2nd order upwind numerical scheme led to bad convergence of solution. This can indicate that solution is not grid-independent (mesh is not fine enough); effect of distorted cells cannot be ruled out, too. There is also a possibility, that the flow is unsteady which was not discovered when large numerical dissipation of the 1st order numerical schemes damped the flow disturbances. In fact, behaviour of the monitored temperatures supports such conclusion; see Fig. 10 and Fig. 11.

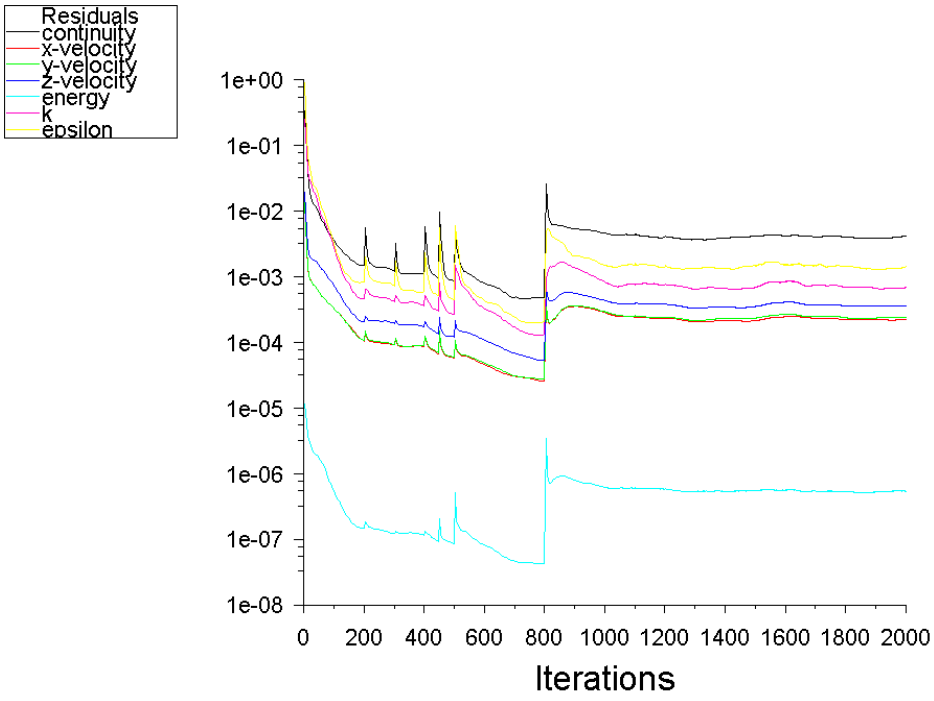

Fig. 9: Scaled residuals with switch from 1st to 2nd order upwind methods after 800 iterations.

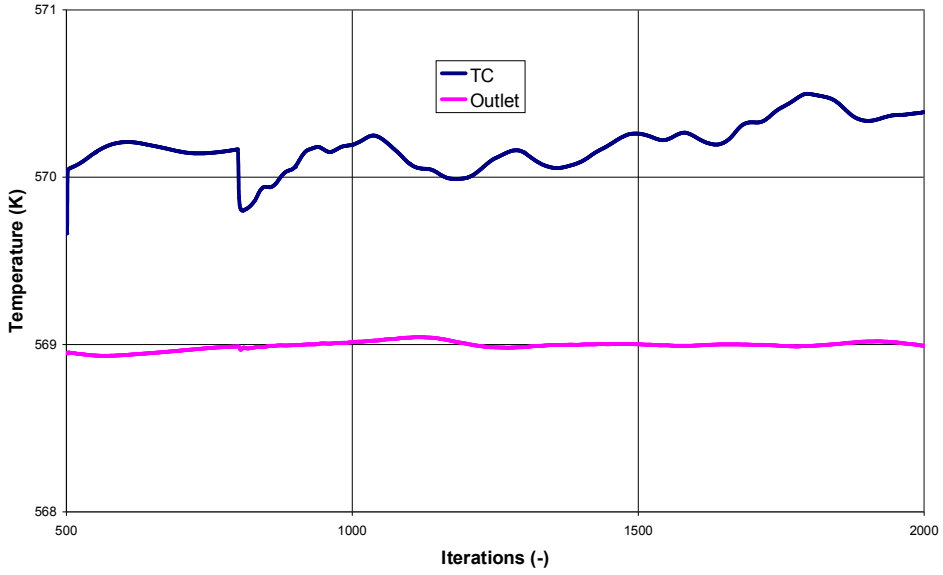

Fig. 10: TC and outlet temperatures during iterations (steady state computations).

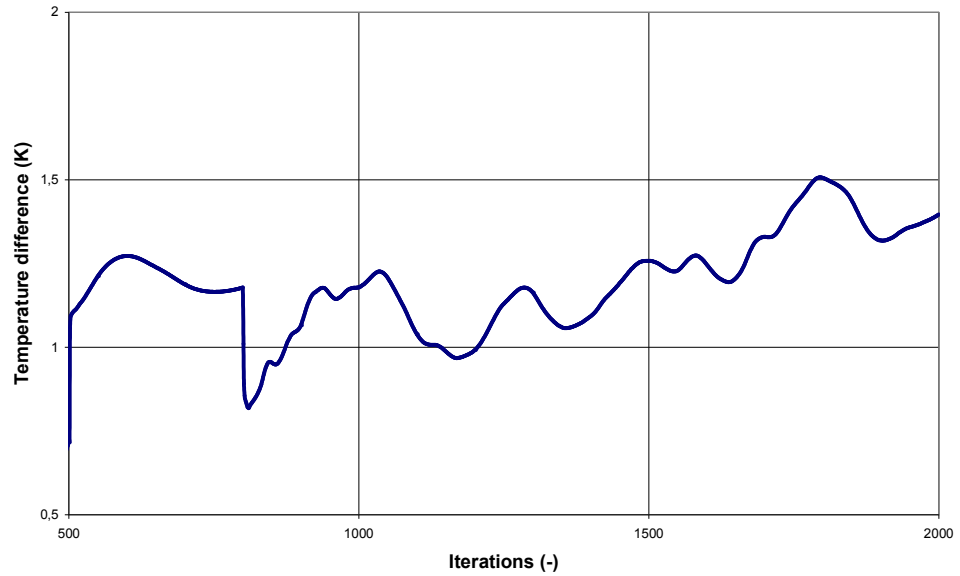

Fig. 11: Temperature difference $T_{TC} - T_{outlet}$ during iterations (steady state computations)

4. 3. Unsteady computations

On the basis of results of steady state computations it was decided to perform unsteady computations starting from the situation after 2000 iterations. Time step of 0.01 s was used which required some 70 iterations in order to reach the prescribed convergence limit (scaled residuals lower than 10^{-4}). Altogether 5 s of transient were computed and it appears that even after some transitional period the TC temperature moves within some 0.3 K. Outlet temperature is almost steady, see Fig. 12.

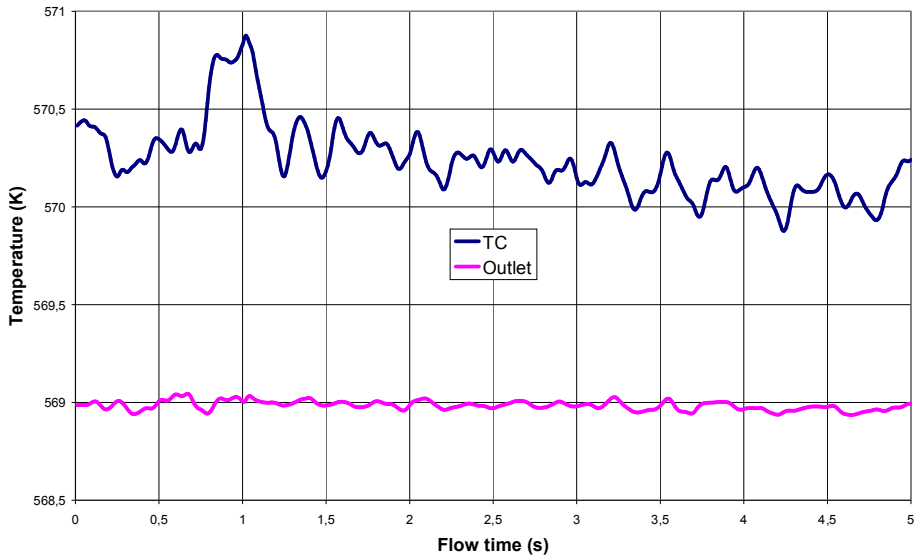

Fig. 12: TC and outlet temperatures during 5 s of unsteady computation.

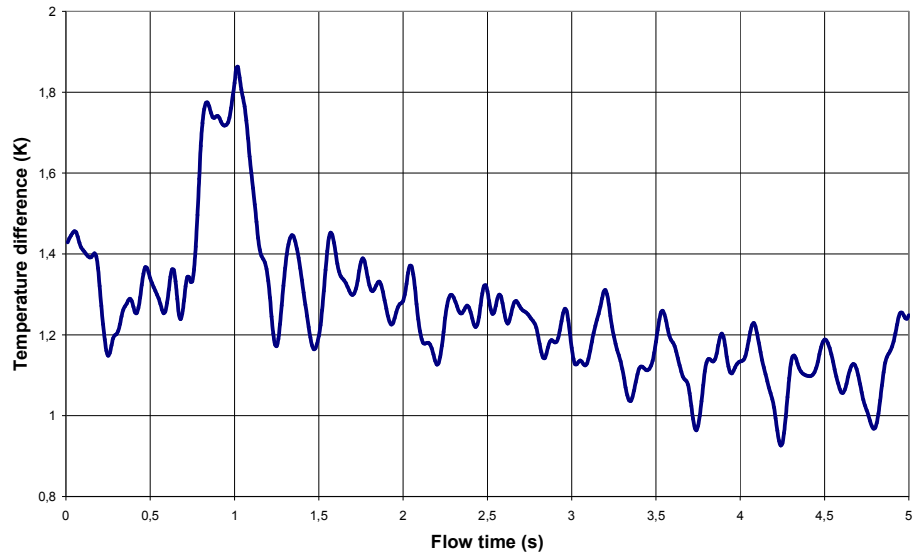

Fig. 13: Temperature difference $T_{TC} - T_{outlet}$ during 5 s of unsteady computations.

It is therefore difficult to produce a single value of temperatures and temperature differences required by benchmark organizers. Even an attempt to find some "average" value of temperature difference failed. Selection of time interval for averaging from 5 s to 0.25 s produced Fig. 14 leading to a possibility that 5 s of transient is not long enough to produce a single average value.

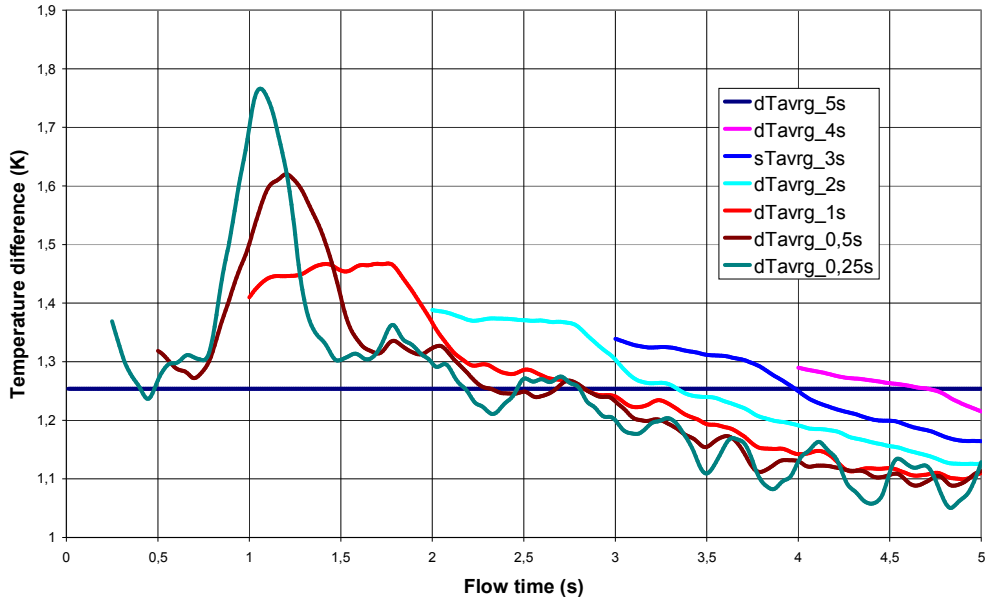

Fig. 14: Temperature difference $T_{TC} - T_{outlet}$ averaged over selected time intervals.

That the flow should be unsteady is quite clear when looking on the geometry of assembly head. The first source of unsteadiness should be the outlet of region of fuel pins which

produces a “bundle” of parallel flows with different velocities. Similar situation is between inlet hexagon and frustum part upstream of the catcher. The catcher itself also represents a possible source of vortex shedding. Finally, unsteady local vortices could be present around the thermocouple.

In this context it can be interesting to know, if the unsteadiness of TC temperature is a local phenomenon, or is convected from some of the mentioned sources upstream. Comparison of TC and outlet area averaged temperatures with local temperatures at selected points on the assembly vertical axis leads to a conclusion, that probably some local phenomena (even possibly artificial due to computational mesh and/or numerical schemes) are the prevailing source of the unsteadiness.

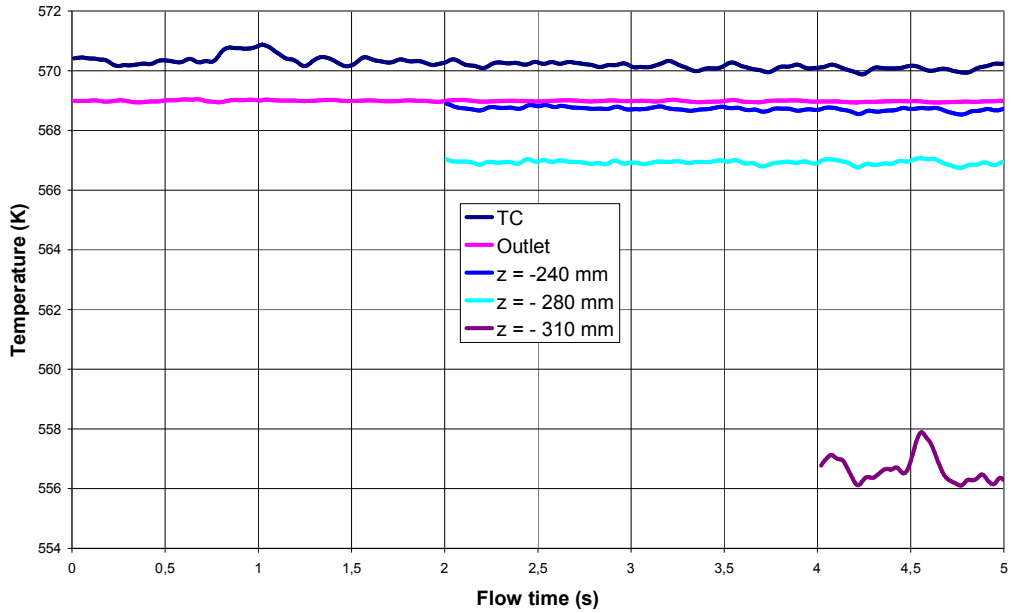

Fig. 15: Temperatures at selected points on assembly vertical axis as compared with averaged TC and outlet temperatures (z = - 310 mm is inlet of the cylindrical part with the catcher, z = -280 mm is catcher inlet and z = -240 mm is catcher outlet; z = 0 mm corresponds to assembly outlet).

5. CONCLUSIONS

Our simplified approach to the VVER-440 head benchmark has several issues which must be addressed in the next phase of FLUENT 12 code validation: effect of separation of the computational domain into two regions (is our inlet region long enough that the outlet boundary condition does not adversely affect the boundary profile even if spacers are included? do spacers affect significantly the thermocouple temperature?), the extent to which the cells with high ESS affect the thermocouple temperature, and the length of the unsteady computations (is the 5 s transient long enough to reach some “statistically steady state”? does such state exist?). Next steps of our validation procedure will therefore include improvement and optimization of the computational mesh in the outlet region on the basis of examination of present results, and detailed study of the questions mentioned above.